The SRG OncoRat®; A Rag2/Il2rg double-knockout rat supports enhanced precision-medicine based cancer studies.

Bisoye Towobola Adedeji[1], Fallon K. Noto[1], Sam Moody[1], Valeriya Steffey[1], Chris Brenzel[1], Jack Crawford[1], Goutham Narla[2], B. Mark Evers[3], Tseten Yeshi Jamling[1]

1 Hera Biolabs, Inc. Lexington, KY 2 Division of Genetic Medicine, The University of Michigan, Ann Arbor, MI 3 Markey Cancer Center, University of Kentucky, Lexington, KY

Abstract

- The SRG™ rat is a Rag2-/- Il2rg -/- double KO on the Sprague Dawley strain resulting in immunodeficiency caused by loss of mature T, B, and circulating NK cells
- The SRG™ *OncoRat*® supports the growth of a wide variety of human cancer cell lines, including those with poor take rate or growth kinetics in immunodeficient mouse models, such as VCaP and LNCaP
- Larger blood volume of the rat facilitates weekly blood sampling for biomarker analysis, such as PSA for prostate cancer
- Larger size of the rat allows for bigger tumors, resulting in more tissue for downstream analyses.
- Fine needle biopsies can be collected weekly from VCaP tumors without affecting tumor growth for assessing protein expression, providing a method for in-life pharmacodynamic analyses during efficacy studies
- Larger tumor volumes, allowing for serial fine needle aspirate biopsy for PK, PD and molecular analysis in the same animal throughout the course of the study without significantly affecting normal tumor growth.
- Larger tumor volumes also enabled the use of fewer animals for studies, allowed for faster timelines to drug efficacy data, and reduced the need for serial passaging to generate enough tissue; Limiting genomic divergence from the parental tumor tissue.
- The SRG Oncorat can be predictive of drug efficacy when using precision medicine approaches in advanced cancer care.

Materials and Methods

Tumor growth kinetics and Biopsy: Commercially acquired Human cancer cell lines were thawed, cultured, passaged and harvested in preparation for inoculation. 6 SRG rats per cell line were inoculated with 0.25mL cell suspension mixed just prior to inoculation, 1:1 with 10mg/mL Matrigel for a total volume of 0.5mL and 5mg/mL final concentration. The mixture was injected subcutaneously into the shaved flank of the SRG rats. The 22RV1 cell line was inoculated at 5 million cells per rat, while VCaP and LNCaP cells were inoculated at ten million cells per rat. Three times weekly tumor measurements were taken, with tumor volumes calculated using (L X W^2)/2. Three times weekly body weights measurements and daily general health monitoring was performed through out the studies.
Histology: Harvested tumor tissue fixed in 10% neutral buffered formalin was processed, paraffin embedded, sectioned and H&E stained. Sectioned samples were also stained for the androgen receptor (AR) biomarker. One and two cores biopsy of the tumors were collected weekly for four weeks. Biopsy was performed aseptically by fine needle aspiration, using 21G needle attached t a 10m syringe.
Blood sampling: Weekly blood sampling for serum was done by venipuncture for Prostate specific antigen (PSA) analysis.
Transplantation of PDX tissues: Non-small cell lung cancer PDX tumor fragments were obtained fresh from patients at the Markey Cancer Center through the University of Kentucky Biospecimen Procurement and Translational Pathology Shared Resource Facility under IRB 17-0513-P3K. Each tissue was cut into 2mm x 2mm x 2mm pieces and immediately implanted subcutaneously using a trocar into SRG rats or NSG mice. For serial transplants, tumors were removed aseptically and cut into 2mm x 2mm x 2mm pieces and transplanted, cryopreserved, flash frozen, or fixed in 10% NBF.
Genomic Analysis: DNA extracted from PDX tissue using was sent to the University of Michigan MMGL-Molecular Genetics core facility for genomic analysis.
Histology: PDX tissue fixed in 10% neutral buffered formalin was processed, paraffin embedded, sectioned and H&E stained by IDEXX.
PDX Efficacy Studies: PDX tissue grown in SRG rats was cryopreserved, then implanted into 3 NSG mice, then serially implanted into 16 NSG mice. Ten tumor-bearing NSG mice were enrolled into one of two treatments: 1) Vehicle control: 0.9%NaCl 10ml/kg, IP twice weekly or 2) Cisplatin 2.5mg/kg, IP twice weekly + Docetaxel 10mg/kg, IP once weekly. For the subsequent PDX efficacy study, tumor tissue grown in an SRG rat was cryopreserved, then implanted into 40 NSGs. Six tumor-bearing mice were enrolled into each of 3 treatment groups: 1) vehicle control (0.5% glucose, 0.2 M HCL in 0.9% NaCl) 2) 50mg/kg Crizotinib in vehicle control, or 3) 60mg/kg Cabozantinib suspended in 0.01M HCl in 0.9% NaCl. All animals were dosed once daily by oral gavage for 28 days. Plasma was collected 2 hours after the terminal dose. Half of each tumor was fixed in 10% NBF for histology and the other half flash frozen for molecular characterization. Five additional tumor-bearing mice were administered either a single dose of vehicle (2 mice) or Cabozantinib (3 mice). At 2 hours post-dose, plasma was collected, and tumor was flash frozen for analysis.

Results

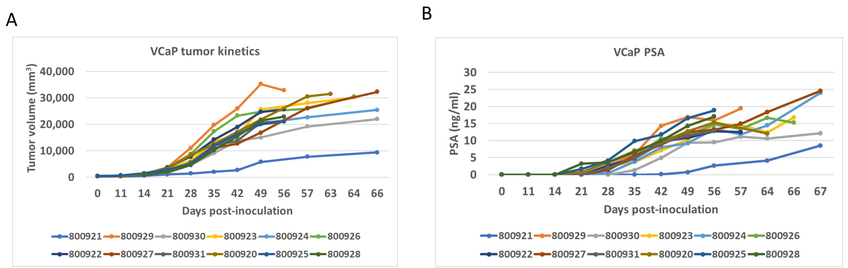

Figure 1: VCaP Tumor volume kinetics, PSA over time, histology of tumor samples and FNA biomarker analysis. A.) Individual lines showing individual tumor growth kinetics. B.) Individual lines showing PSA levels in individual rats over the course of tumor growth. Tumor growth rate correlates with blood PSA levels C.) VCaP Tumor IHC. Sections showing representative H&E staining AP and PSA demonstrating robust presence of positive biomarkers. D.) Fine needle biopsies taken from VCaP tumors once weekly for 4 weeks were assessed for PSA and AR expression. Data shown for animal 800931.. E.) VCaP tumor growth kinetics showing One or two cores weekly FNA biopsy points with no apparent effect on tumor growth.

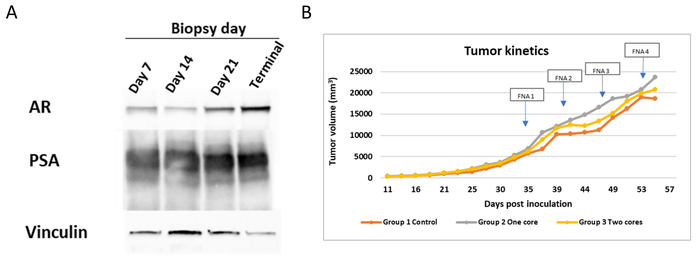

Figure 2: A.) Fine needle biopsies taken from VCaP tumors once weekly for 4 weeks were assessed for PSA and AR expression. Data shown for animal 800931. B.) VCaP tumor growth kinetics showing One or two cores weekly FNA biopsy points with no apparent effect on tumor growth.

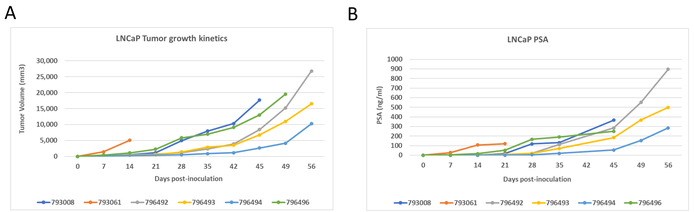

Figure 3: LNCaP Tumor volume kinetics, PSA over time and histology of tumor samples. A.) Individual lines showing individual tumor growth kinetics. B.) Individual lines showing PSA levels in individual rats over the course of tumor growth.

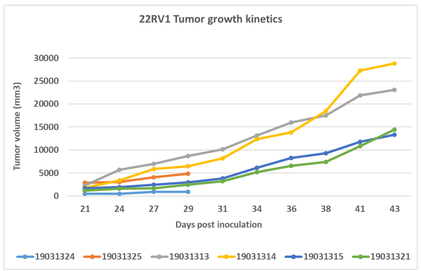

Figure 4: 22RV1 PDX tumor kinetics and PSA levels over time. Individual lines showing individual tumor growth kinetics, tumor engraftment rate was 100%.

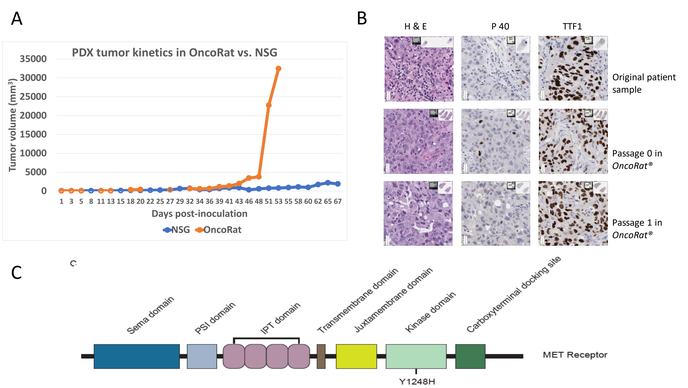

Figure 5: NSCLC PDX patient 3010 tumor growth kinetics, histology and genetic mutation identification. A.) NSCLC PDX tumor kinetics in the OncoRat and NSG mouse. Tumor growth kinetics of the same PDX sample grown in OncoRat and NSG mouse. B.) IHC staining for H&E, P40, and TTF1 in original patient tumor sample, first passage in the SRG rat, and second passage in the SRG rat. C.) Schematic of MET receptor depicting the likely pathogenic mutation Y1248H found in patient 3010.

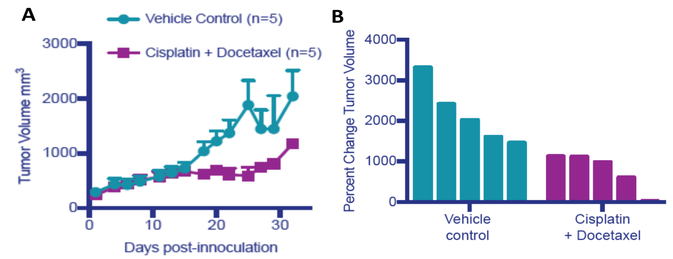

Figure 6: Patient 3010 NSCLC PDX efficacy study with standard of care therapeutics. A) Tumor growth curve and B) waterfall plot of patient derived NSCLC tumors (3010) treated with vehicle control or 2.5mg/kg Cisplatin twice weekly in combination with 10mg/kg Docetaxel once weekly.

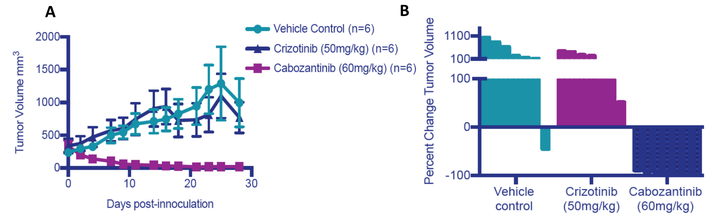

Figure 7: Patient 3010 NSCLC PDX efficacy study with targeted treatment based on genomic analysis. A) Tumor growth curve and B) waterfall plot of patient derived NSCLC tumors treated with vehicle control, 50m/kg Crizotinib, or 60mg/kg Cabozantinib daily.

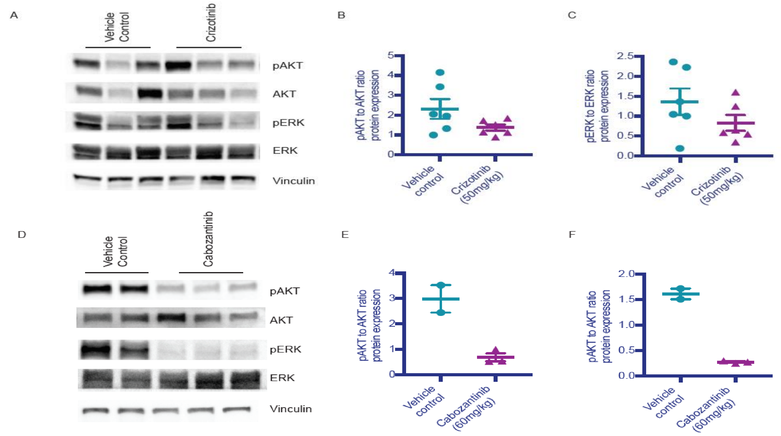

Figure 8: Molecular analysis of PDX targeted treatment efficacy study. A) Western Blot analysis for phosphorylated AKT, AKT, phosphorylated ERK, ERK, and Vinculin in PDX model treated with vehicle control or Crizotinib. Quantification of densitometry depicting ratio of B) phosphorylated AKT to total AKT and C) phosphorylated ERK to total ERK. D) Western blot analysis for phosphorylated AKT, AKT, phosphorylated ERK, ERK, and Vinculin in PDX model treated with one dose of vehicle control or Cabozantinib. Quantification of densitometry depicting ratio of E) phosphorylated AKT to total AKT and F) phosphorylated ERK to total ERK.

Conclusions

1. The OncoRat® SRG™ has superior tumor take rates and growth kinetics, providing a more efficient model for drug efficacy studies.
2. The OncoRat® SRG™ support the growth of PDX samples which exhibit faster growth kinetics compared to growth of the same samples in NSG mice. It also produces sufficient PDX tissue in a single passage for downstream efficacy studies.
3. The OncoRat may be predictive of drug efficacy using precision medicine approaches for advanced cancer patients.

Acknowledgements

We would like to thank Dr. Goutham Narla for the critical insight and data analysis. We would like to thank the Markey Cancer Center and University of Kentucky Biospecimen Procurement and Translational Pathology Shared Resource Facility for the fresh PDX samples. Sequencing studies were carried out with the support of the Michigan Medical Genetics Laboratories in the Department of Pediatrics and the support of C.S. Mott Children's Hospital.

Presenter contact: btowobola@hearbiolabs.com